LA-UR-90-668

CONF-9004136--3

Received by OSTI

MAR 05 1990

Los Alamos National Laboratory is operated by the University of California for the United States Department of Energy under contract W-7405-ENG-36.

LA-UR--90-668

DE90 007505

TITLE: MUZZLE SHUNT AUGMENTATION OF CONVENTIONAL RAILGUNS

AUTHOR(S): Jerald V. Parker

SUBMITTED TO: Fifth Symposium on Electromagnetic Launcher Technology
Sandestin Conference Center
Destin, Florida

2-5 April 1990

Los Alamos Los Alamos National Laboratory
Los Alamos, New Mexico 87545

FORM NO. 836 R4
ST. NO. 2629 5/81

MUZZLE SHUNT AUGMENTATION OF CONVENTIONAL RAILGUNS*

Jerald V. Parker
Los Alamos National Laboratory
Physics Division, MS E526
Los Alamos, NM 87545

Abstract

Augmentation is a well-known technique for reducing the armature current and hence the armature power dissipation in a plasma armature railgun. In spite of the advantages, no large augmented railguns have been built, primarily due to the mechanical and electrical complexity introduced by the extra conductors required. It is possible to achieve some of the benefits of augmentation in a conventional railgun by diverting a fraction ϕ of the input current through a shunt path at the muzzle of the railgun. In particular, the relation between force and armature current is the same as that obtained in an n-turn, series-connected augmented railgun with $n = 1/(1-\phi)$. The price of this simplification is a reduction in electrical efficiency and some additional complexity in the external electrical system. Additions to the electrical system are required to establish the shunt current and to control its magnitude during projectile acceleration. The relationship between muzzle shunt augmentation and conventional series augmentation is developed and various techniques for establishing and controlling the shunt current are illustrated with a practical example.

Introduction

The series augmented railgun illustrated in Fig. 1 has been studied in laboratory devices by Fikse, et.al.[1] and by Shrader, et.al[2]. Neither investigation found any particular advantage for the augmented configuration compared to a conventional railgun. This conclusion is supported by a comparative study performed by Kotas, et.at.[3] who found that increased resistive losses in the augmenting rails offset any advantages gained from reduced driving current. A study of the structural design issues in augmented railguns by Wellman and Schuler [4] showed that practical augmentation is limited to small n (~2 or 3) by transverse forces that increase with n. As a consequence of such experimental and theoretical work, augmentation has not been utilized in any large scale electromagnetic launcher devices.

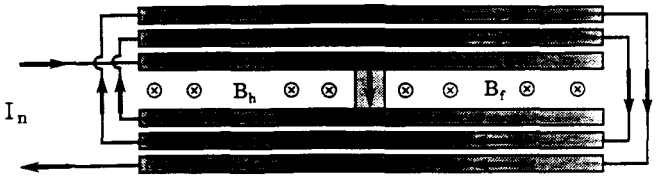

Figure 1. Series augmented railgun (n = 3)

*Work supported by the U. S. Dept. of Energy

It is important to realize, however, that the validity of these conclusions is limited to the particular experimental condition investigated or the particular system model analyzed. For example, [3] treated a low velocity (3 km/s) railgun for which circuit resistive losses are a major determinant of overall system efficiency. A substantially different conclusion is reached for the case of a high velocity, plasma armature railgun where the major performance loss results from material ablated into the railgun bore by power dissipation in the armature plasma. Parker [5] suggests that a moderate level of augmentation (n = 2 or 3) may be sufficient to eliminate bore ablation in railguns with high performance ceramic insulation. In this case there is the potential for a large payoff from a modest level of augmentation.

The remaining obstacle to the application of augmentation to a plasma armature railgun is the mechanical and electrical complexity inherent in multiple internal conductors. This complexity translates into increased construction and maintenance costs and reduced reliability. Our purpose in this paper is to describes an alternative technique that provides most of the advantages of series augmentation without the requirement for additional conductors.

Analysis

The proposed technique, which we designate Muzzle Shunt Augmentation (MSA), is illustrated in Fig. 2. It consists of a conventional railgun with a shunt circuit connected across the muzzle. The shunt may be a short-circuit or it may contain various components as discussed in the next section. The equivalence between the geometry shown in Fig.2 and the series agumented railgun of Fig. 1 is apparent if one examines the internal magnetic fields and currents.

For the purposes of this analysis the series augmented railgun will be treated as a ideal device with perfectly conducting rails that are tightly coupled magnetically. In this approximation each set of internal conductors has the same inductance gradient, L_0'.

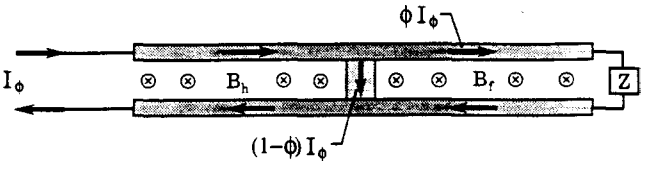

Figure 2. A conventional railgun with shunt impedance Z connected across the muzzle.

Then the magnetic field in the railgun bore is given by

$$B_h = n L_0' I_n/h \quad \text{(behind armature)} \quad (1)$$

$$B_f = (n-1) L_0' I_n/h \quad \text{(before armature)} \quad (2)$$

where h is the bore height. The force on the armature is the product of the armature current(I_n), armature length(h) and the *average* magnetic field at the armature.

$$F_n = I_n h (B_h+B_f)/2 = {}^1/_2 (2n-1) L_0' I_n^2 \quad (3)$$

For the MSA case the magnetic fields are given by

$$B_h = L_0' I_\phi/h \quad (4)$$

$$B_f = \phi L_0' I_\phi/h \quad (5)$$

where ϕ is the fraction of the input current that is diverted from the armature into the shunt at the muzzle. Since the armature current is now $I_a = (1 - \phi) I_\phi$ the force on the armature for the MSA case is

$$F_s = {}^1/_2 (1 - \phi^2) L_0' I_\phi^2 \quad (6)$$

Eqns 1,2 and 3 are formally identical to equations 4,5 and 6 with the following identifications;

$$I_n = I_\phi / n \quad (7)$$

and

$$n = 1 /(1 - \phi). \quad (8)$$

This formal equivalence also holds for the armature current. Substituting eqns 7 and 8 into the expression for the MSA armature current (Eqn. 6) yields

$$I_a = (1 - \phi) I_\phi = I_\phi/n = I_n$$

The practical meaning of this equivalence is that the MSA railgun provides the same reduction in armature current (and armature power dissipation) as the series augumented railgun. The analysis also highlights two significant differences. The first difference, shown in eqn. 7, is that the series augmented railgun acts as a transformer, reducing the required power supply current by $1/\sqrt{2n-1}$ and increasing the required power supply voltage by $\sqrt{2n-1}$. In contrast the MSA railgun has the same power supply requirements as a conventional railgun. A second difference lies in the nature of the parameters n and ϕ. Eqn. 8 is only valid for the discrete values of ϕ ($^1/_2$, $^2/_3$, $\cdots$) that yield integer values of n, but the MSA railgun can operate with any value of ϕ from 0 to 1, thus permitting intermediate values of augmentation.

Table I. Comparison of muzzle shunt augmentation and series augmentation at constant force.

Parameter	MSA	Series
Accelerating force	1	1
Armature current	$\frac{\sqrt{1-\phi}}{\sqrt{1+\phi}}$	$\frac{1}{\sqrt{2n-1}}$
Rail-rail voltage	$\frac{1}{\sqrt{1-\phi^2}}$	$\frac{n}{\sqrt{2n-1}}$
Initial stored energy	$\frac{\phi^2}{1-\phi^2}$	$\frac{(n-1)^2}{2n-1}$
Transverse force[f]		
Final stored energy	$\frac{1}{1-\phi^2}$	$\frac{n^2}{2n-1}$
Transverse force[b]		
Input current	$\frac{1}{\sqrt{1-\phi^2}}$	$\frac{1}{\sqrt{2n-1}}$
Breech voltage	$\frac{1}{\sqrt{1-\phi^2}}$	$\sqrt{2n-1}$
Power input	$\frac{1}{1-\phi^2}$	1

f-in front of armature, b-behind armature

There are other , less obvious, differences between the MSA and series augmented railgun. Some of these differences are shown by the comparisons presented in Table I. In order to make a meaningful comparison between the MSA and series augmented railgun it is necessary to fix one performance parameter. In Table I the fixed parameter is the driving force, F_0. For example, the current scaling relations at fixed F_0 are,

$$I_n = I_0 / \sqrt{2n-1} \qquad \text{Series augmented}$$

$$I_\phi = I_0 / \sqrt{1-\phi^2}, \qquad \text{MSA}$$

where I_0 is the current that produces a driving force of F_0 ($=^1/_2 L_0' I_0^2$) in a conventional railgun ($n=1$ or $\phi=0$). Only the coefficients are given for each entry in Table I. The physcal result can be recovered by multiplying this coefficient times the appropriate expression for a conventional railgun, e.g. breech voltage($L_0' I_0 v$), power input($L_0' I_0^2 v$),etc.

The entries above the dashed line in Table I are all formally equivalent as described above. The last three entries are not equivalent and represent real differences between MSA and series augmentation. The input current expessions differ by a factor of n due to the transformer action discussed earlier. The breech voltage for a series augmented railgun increases inversely as the current decrease so that their product, the power input, is constant and equal to the power input to a conventional railgun. This

is not the case for the MSA railgun. Here the input current increases as ϕ increases to maintain a constant accelerating force and the breech voltage also increases. The result is an increase in power input for constant power delivered to the projectile, i.e. decreased efficiency.

The reason for this inefficiency is easily understood by comparing the configurations shown in Figs. 1 and 2. The magnetic flux in front of the projectile in the series augmented railgun is trapped by the rail-to-rail connections and forced to flow back into the breech region as the projectile moves forward. None of the energy associated with this flux is lost. In contrast, the flux ahead of the projectile in the MSA railgun, which must decrease as the projectile pushes it out of the railgun, cannot return to the breech region and must be dissipated. The resulting energy loss is supplied by an increased power input at the breech.

The lower efficiency of MSA restricts its practical use to small values of ϕ. At $\phi = 0.5$, corresponding to $n = 2$, the power requirement is 33% greater than a conventional railgun and at $\phi = 0.67$ ($n = 3$) it is 80% greater. Unless some of this extra energy can be recovered (see discussion below) the MSA approach quickly becomes unattractive.

Practical Application

With the analytical picture well in hand the next question is the practicability of MSA. Three elements are need for a successful MSA railgun; a shunt circuit, a means to establish the shunt current and a means to control the value of ϕ during projectile acceleration. The shunt circuit is straightforward. Many railguns already employ snubbing resistors at the muzzle so methods exist to implement the shunt circuit.

Establishing and controlling the shunt current is a bit more difficult. To illustrate some potential methods we will consider a illustrative railgun design and calculate the performance expected for several MSA configurations. The baseline railgun design is presented in Table II. For computational convenience the muzzle shunt circuit is modeled as a series connected resistor, capacitor and inductor. Other circuit configurations may also be of practical interest.

Table II. Railgun Design for MSA Examples.

Capacitor Bank	**Railgun**
C_B = 0.033 F	L_0' = 0.35 μH/m
L_B = 7.6 μH	R' = 50 μΩ/m
R_B = 50 μΩ	l = 15 m
	D = 6 cm
Armature-Projectile	
V_A = 220 V	**Initial Conditions**
R_A = 100 μΩ	v_i = 2.0 km/s
M_P = 175 g	V_B = 30 kV

The baseline railgun design assumes a plasma armature. It is modeled as a fixed voltage of 220 volts in series with a 100 μohm resistor. The armature model is important because magnetic flux leakage through the armature has a signficant impact on the shunt current.

The simplest way to establish current in the shunt is to use the armature voltage to induce a current in the muzzle circuit. Figure 3 show the calculated current waveforms for this situation. The shunt component values are R_S=0.1 mΩ, L_S=0.1 μH, and C_S=1000 F. The capacitance is set to 1000 F so that it has no effect on the calculation. The values of L_S and R_S effectively short circuit the muzzle.

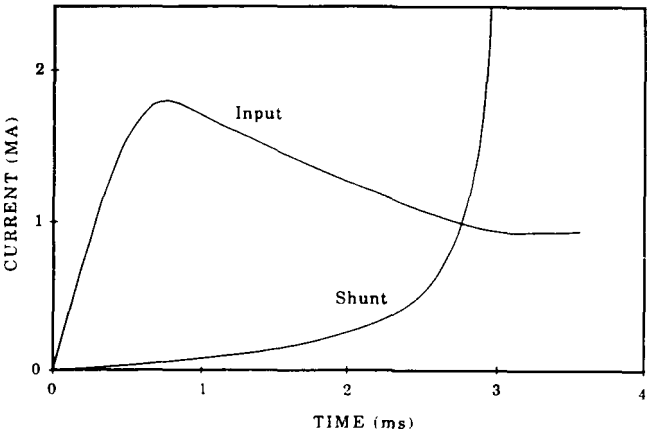

Figure 3. Current waveforms when the shunt circuit is charged only by the armature voltage.

Two practical problems are immediately apparent in Fig. 3. First, the shunt current increases continuously so that ϕ varies from 0 to > 1. Second, short circuiting the muzzle has trapped the flux in the muzzle circuit so that the shunt current rises exponentially as the projectile approaches the muzzle. As the shunt current becomes equal to the input current the driving force falls to zero resulting in poor efficiency.

A effective way to establish the shunt current is to turn on the capacitor bank before the projectile enters the railgun. Figure 4 shows the current waveforms obtained when the capacitor bank is discharged 450 μs before the projectile contacts the rails. For the first 450 μs the capacitor bank charges the storage inductor and the railgun inductance in series. When the projectile reaches the rails the low resistance armature becomes the primary path for the remaining capacitor bank current and the shunt current remains nearly constant. At late time current amplification again causes the shunt current to grow rapidly if the shunt resistance is small. The growth rate can be controlled by introducing additional resistance into the shunt circuit as shown by the family of curves in Fig. 4.

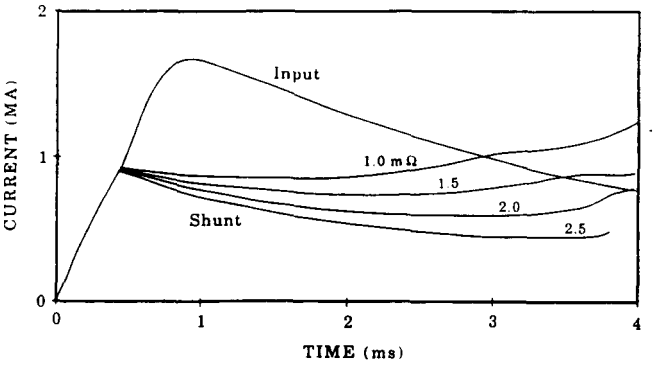

Figure 4. Current waveforms showing precharging of the shunt current and reduction of current amplification using a shunt resistor.

The largest value of shunt resistance shown in Fig. 4 , 2.5 mΩ, is sufficient to keep the shunt current below the input current thoughout the launch but the current waveform is not a good approximation to constant ϕ.

Current amplification can also be controlled by an inductor or capacitor in the shunt circuit. Figure 5 shows the effect of introducing progressively larger values of inductance. The current gain is reduced but only when a large inductance is used (comparable to the railgun inductance of 5.25 μH) and this seriously reduces the operating current.

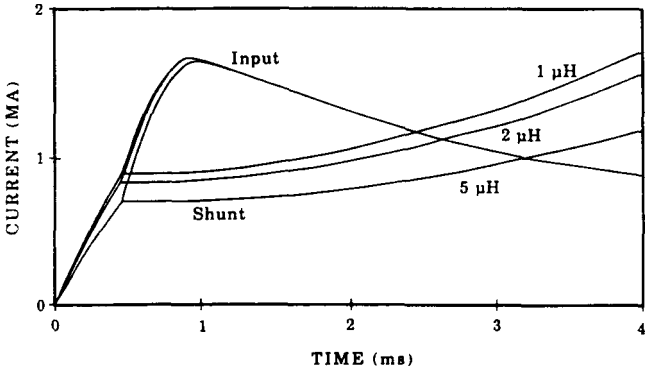

Figure 5. Calculated waveforms for several values of shunt inductance.

Fig. 6 presents the calculated waveforms for a series of shunt capacitors. The capacitor effect depends on charge rather than current and is strongest at late time. The behavior of the current waveforms for resistance and capacitance are somewhat complementary, suggesting that a combination of the two might give better control of the waveform. Figure 7 treats the case of a series resistor and capacitor. The resistance is set at 1.8 mΩ based on the early time behavior in Fig. 4 and the capacitor is adjusted to obtain the best waveform. A capacitance of 5.0 F produces a good approximation to ϕ = 0.5 operation. Further optimization is possible by adjusting both R and C but the present result is sufficient to illustrate the principle.

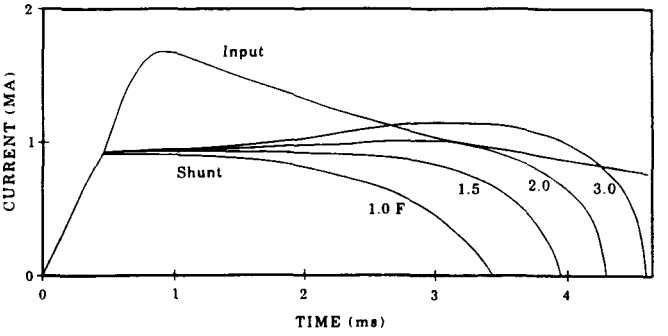

Figure 6. Current waveforms for several values of shunt capacitance.

How practical is this approach? The 1.8 mΩ resistor must dissipate about 2.4 MJ. This is certainly feasible using a high resistivity, sheet metal resistor although some attention would be required keep the inductance low. The capacitor reaches a maximum voltage of 470 volts so the 5 F bank could be realized using electrolytic capacitors. The stored energy in the shunt capacitor bank is 550 kJ. The required bank is not small but it is substantially smaller than the 15 MJ primary capacitor bank.

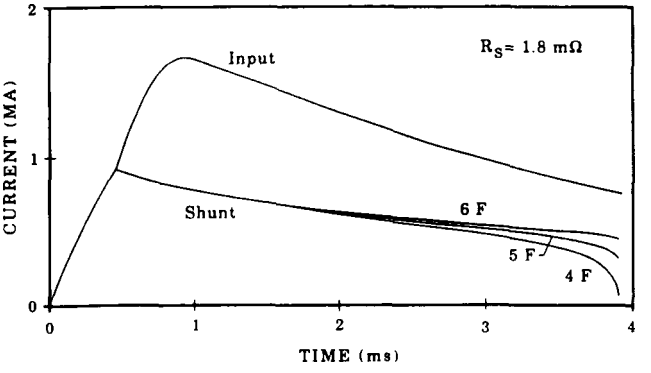

Figure 7. MSA current waveforms for a series resistor and capacitor in the shunt circuit

Using the main capacitor bank to establish the shunt current has a potentially serious drawback. When the main bank is discharged without a projectile in the railgun the breech voltage is determined by the ratio of railgun inductance to total circuit inductance. In the example given above this voltage is 12.3 kV. Usually the railgun bore must be under a good vacuum or at atmospheric pressure to withstand such a high voltage. Neither condition is currently considered practical for operation at 6+ km/s.

A refinement of the MSA circuit, shown in Fig.8, allows the shunt current to be established independently of the main

Figure 8. Refinement of the basic MSA circuit providing independent control of the precharge current.

capacitor bank. In this configuration a muzzle capacitor, C_M, is precharged to a voltage the railgun can tolerate, generally 2 to 3 kV, and then discharged through switch S_2 and diode D before the projectile enters the railgun. When the projectile enters the railgun switches S_1 and S_3 are closed and the circuit operates as described earlier.

For some designs it may be feasible to use the same capacitor needed for waveform control to provide the precharge. In this case the muzzle capacitor should not be electrolytic because its potential will reverse during operation.

Discussion

The cost and benefits of MSA operation can be evaluated by comparing the example case shown in Fig. 7 (R_s = 1.8 mΩ, C_s = 5 F) with the calculated performance for conventional operation (R_s=∞). The MSA example has an exit velocity of 5.9 km/s. To achieve this same velocity in the conventional configuration the initial charge on the capacitor bank must by reduced from 30 kV to 24.2 kV. Thus MSA operation requires ~ 54% higher input energy.

The benefit obtained for this extra energy investment is a reduction in armature power dissipation and ablation. The peak armature power dissipation for the MSA example is 270 MW compared to 525 MW for conventional operation. The effect of this power reduction on wall ablation can be quite dramatic when a high performance ceramic insulator material is employed in the railgun.

According to [5] insulator performance can be assessed in terms of the power per unit area incident on the insulator multiplied by the square root of the exposure time. Following that analysis one can calculate the ablation expected in the MSA and conventional railgun for an advanced ceramic insulator.

For comparison purpose consider pyrolytic BN whose threshold for ablation damage is 4.2 x 10^7 W $\sqrt{s}/m^2$. In the MSA example this threshold is exceeded for only 655 μs and the peak exposure is only 25 % over threshold. The calculated insulator ablation during the launch is 0.072 grams.

For the conventional railgun case the threshold is exceeded for 2200 μs, the peak exposure is 244 % of threshold, and the ablated mass is 3.2 grams. The initial armature mass in this example is about 0.7 grams (CH_2 plasma). Augmented operation adds only 10 % to the armature mass during launch whereas conventional operation increases the armature mass by a factor of 5.6.

The example presented above is far from an optimized railgun design. The propulsive force (and efficiency) of an MSA railgun can be maximized by tailoring the current waveform and the shunt fraction ϕ so that the insulator is always operated just below its ablation threshold. As advanced ceramic insulator materials are incorporated into the next generation of railguns the MSA technique may play an important role in overcoming the 6 km/s performance limit of present plasma armature railguns.

References

[1] D. A. Fikse, J. L. Wu, and Y. C. Thio, "The ELF-I Augmented Electromagnetic Launcher", IEEE Trans. on Magnetics, MAG-20, pp 287-290, March 1984

[2] J. E. Shrader, A. J. Bohn, and J. G. Thompson, "Railgun Experimental Results Due To Varying Bore and Arc Materials, and Varying the Number of Barrel Turns", IEEE Trans. on Magnetics, MAG-22(6), pp 1739-1741, November 1986

[3] J. F. Kotas, C. A Guderjahn, and F. D. Littman, "A Parametric Evaluation of Railgun Augmentation", IEEE Trans. on Magnetics, MAG-22(6), pp 1573-1577, November 1986

[4] G. W. Wellman and K. W. Schuler, "Structural Consequences of Railgun Augmentation", IEEE Trans. on Magnetics, MAG-25(1), pp 593-598, January 1988

[5] J. V. Parker,"Why Plasma Armature Railguns Don't Work (and What Can Be Done About It)", IEEE Trans. on Magnetics, MAG-25(1), pp 418-424, January 1988